Desalination and Water Treatment
www.deswater.com

doi: 10.5004/dwt.2023.30057

313 (2023) 186–195
November

Synthesis of metallic nanoparticles and its application in adsorption of metanil yellow and Rhodamine B from aqueous solutions

Sultan Alam[a], Rahat Ullah[a], Najeeb ur Rahman[a], Muhammad Ilyas[a], Shakir Ullah[a], Muhammad Zahoor[b,*], Muhammad Naveed Umar[c], Riaz Ullah[d], Essam A. Ali[e]

[a]*Department of Chemistry, University of Malakand, Chakdara, Dir Lower, KPK 18800, Pakistan, dr.sultanalam@yahoo.com (S. Alam), rahatullah186@gmail.com (R. Ullah), nrnajeeb@yahoo.com (N. ur Rahman), michemist93@gmail.com (M. Ilyas), shakirullah185@gmail.com (S. Ullah)*
[b]*Department of Biochemistry, University of Malakand, Chakdara, Dir Lower, KPK 18800, Pakistan, email: mohammadzahoorus@yahoo.com*
[c]*Department of Chemistry, University of Liverpool, UK, email: m.naveed-umar@liverpool.ac.uk*
[d]*Department of Pharmacognosy, College of Pharmacy, King Saud University, Riyadh, Saudi Arabia, email: rullah@ksu.edu.sa*
[e]*Department of Pharmaceutical Chemistry, College of Pharmacy King Saud University Riyadh Saudi Arabia, email: esali@ksu.edu.sa*

Received 6 September 2023; Accepted 14 October 2023

ABSTRACT

Metanil yellow and Rhodamine B are the emerging dyes having applications in a number of sectors. As with every dye during their utilizations, some of its portion is lost into environment in effluents leading to numerous health complications in animals and plant. Herein, mono-metallic Cu and bimetallic Cu–Ni nanoparticles were prepared for the efficient removal of the mentioned dyes from textile effluents. SEM, XRD, EDX and FTIR techniques were used to study their surface morphology, crystalline or amorphous nature, elemental composition and surface functionalities, respectively. The copper nanoparticles were used as adsorbent for metanil yellow adsorption whereas for rhodamine the bimetallic nanoparticles were used as adsorbent. Batch adsorption test in line with various kinetics and isotherm models were utilized to determine the adsorption parameters and underlying mechanisms. For metanil yellow the equilibrium was achieved within 30 min whereas for Rhodamine B equilibrium was reached in 12 min correspondingly when contacted with mono and bimetallic particles of copper. Best fits for the kinetics and isotherm data were respectively obtained with pseudo-second-order model and Langmuir model. The maximum adsorption capacity of Cu nanoparticles was 200 mg/g for metanil yellow whereas for Cu–Ni nanoparticles it was 416 mg/g for Rhodamine B, at 333 K. The thermodynamic studies revealed both the processes to be endothermic, spontaneous, and favorable.

Keywords: Dyes; Pollutants; Kinetics; Isotherms; Thermodynamics parameters

1. Introduction

Out of the three portions of available waters on earth, only a small proportion is drinkable which is also constantly prone to get contaminated with organic and inorganic substances which slowly and gradually have made water unfit for drinking and other uses in some parts of the world. If left unchecked the human population on earth would faces severe water crises in near future. Though the contaminants are added from natural process as well but diverse human activities have worsened the situation further. Among the added contaminants, dyes are a significant category that not only effecting the water quality but also

* Corresponding author.

interfere with photosynthetic activities occurring in water bodies which in some cases leading to suffocation of animals dwelling there. Polluting effects of the dyes is sometime due to their non-biodegradability, gets accumulated in water bodies. Some of the dyes even give rise to more drastic metabolites that are potential carcinogenic or mutagenic compounds causing allergies, skin irritation, etc. [1,2]. In a reported study, Rhodamine B has been found to cause toxicity in oyster larvae and eggs in concentrations greater than 1 mg/L [3]. Metanil yellow is extensively used in the developing countries as a colorant in ice-creams, soft drinks and beverages, coating of turmeric, laddu, spices etc. due to its orange-yellow color. Although the use of metanil yellow as a colorant is not permissible, it is still widely used as a colorant in many food industries. The information regarding basic mechanism of toxicity induced by metanil yellow after ingestion through gastrointestinal tract are very limited. Metanil yellow disrupts the gastric and intestinal secretions, causing necrosis in the glandular and columnar epithelium cells of the stomach and intestine [4,5].

In recent years, various techniques have been developed for the removal of dyes from wastewater, including adsorption, biosorption, coagulation/flocculation, advanced oxidation, ozonation, membrane filtration, etc. [6]. However, adsorption is the most efficient, economic and versatile technique among them [6]. Adsorption techniques have potential in removing organic and inorganic pollutants from water with high efficiency. Carbon based adsorbents comparatively have high specific surface area and are thus more frequently used in solving aqueous pollution problems. In spite of this it also suffers from few disadvantages. However, on the other hand activated carbon is quite expensive, and its regeneration produces additional effluent resulting in considerable loss (10%–15%) of the adsorbent [7]. Recent advancements in nanotechnology have enabled us to fabricate particles of the desired sizes to get maximum uptakes of pollutants from wastewater. Such nano sized adsorbents are more versatile and are considered as alternative of activated carbons.

Nanoparticles finds extensive applications in various fields. Palladium nanoparticles have played their role as remarkable catalyst and adsorbent due to appreciable surface area to volume ratio [8]. Notably, the utilization of metal nanoparticles in technology has exhibited exceptional efficacy and adaptability in addressing emerging pollutants. In the technological and scientific fields, bimetallic nanoparticles have attracted greater attention than their monometallic counterparts in chemical, biological, mechanical, electrical, and thermal capabilities these days. Bimetallic nanoparticles have more surface area than their mono counterparts, which increases their capacities towards adsorption [9].

In the current study, monometallic Cu and bimetallic Co–Mn nanoparticles were synthesized, and characterized were then correspondingly used as adsorbents for metanil yellow and Rhodamine B dyes.

2. Material and methods

2.1. Materials

Nickel sulfate hexa-hydrate ($NiSO_4{\cdot}6H_2O$), copper sulfate penta-hydrate ($CuSO_4{\cdot}5H_2O$), sodium boro-hydride ($NaBH_4$), sodium hydroxide (NaOH), ethanol (C_2H_5OH), and distilled water were the used chemical reagents in this study which were purchased from Sigma-Aldrich, Germany. Metanil yellow and Rhodamine B were also obtained from Sigma-Aldrich. All reagents were used without any further purification.

2.2. Metanil yellow

Acid yellow 36 (Fig. 1), also known as metanil yellow, an azo dye that is used as pH indicator. Though in foods its use is prohibited but still used extensively in some countries as it enhances the visual appearance of various food products. For example, in India, it is commonly used in sweets, beans, and even turmeric due to its distinctive yellow to orange color. Metanil yellow can potentially lead to toxic methemoglobinemia and cyanosis when ingested, and it may also cause allergic dermatitis upon direct skin contact.

2.3. Rhodamine B

Rhodamine B (Fig. 2) is chemical compound often used as a tracer dye in water to track its flow, speed, and direction. Rhodamine dyes are easy to spot because they emit fluorescence, and are detected in a cost-effective way using a fluorometer. Rhodamine B is among the most commonly employed dye, finding widespread uses in various industries such as leather production, paint, textiles, paper, and more. However, these organic dyes may cause serious biological and environmental problems, including the possibility of skin and eyes irritations.

2.4. Characterization

The prepared mono and bimetallic nanoparticles were characterized by scanning electron microscope (SEM Model:

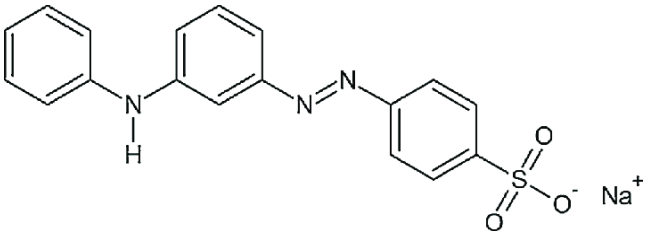

Fig. 1. Metanil yellow structure.

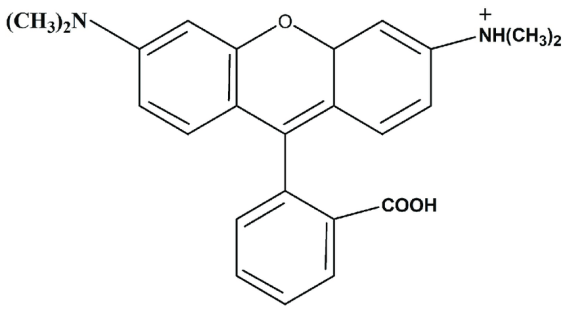

Fig. 2. Rhodamine B structure.

JSM-IT-100), energy-dispersive X-ray diffraction (EDX), XRD (JDX-3532) and FTIR (Cary630).

2.5. Synthesis of nanoparticles

Copper (Cu) nanoparticles were synthesized using a copper precursor prepared by mixing a 2 mmol solution of $CuSO_4 \cdot 6H_2O$ with 1 mmol of $NaBH_4$. The $NaBH_4$ solution in ethanol was sonicated for 1 h prior to mixing followed by stirring on a magnetic stirrer for 10 min. Subsequently, the Cu solution was promptly introduced into $NaBH_4$ solution and stirred for 1 h. After separation and purification of the Cu nanoparticles they were dried in an oven for 5 h and then allowed to cool to the room temperature. The copper nanoparticles were subsequently used as adsorbent for metanil.

For the preparation of copper bimetallic nanoparticles nickel sulphate hexahydrate ($NiSO_4 \cdot 6H_2O$) was reacted with pentahydrate of copper sulphate ($CuSO_4 \cdot 5H_2O$) salts per following detail. An equimolar mixture of the two salts was dissolved in deionized water (1:1 ratio), resulting in a clear solution with a molarity of 0.01. Nitrogen gas (N_2) was bubbled through the solution for 30 min. The sodium borohydride ($NaBH_4$) was then quickly poured into mixture to ensure the chemical reduction and stirred for 30 min. The precipitates formed were washed multiple times with water before being treated with ethanol. The precipitates were the dried at 60°C for 12 h in an oven. The resulting material was used as adsorbent for Rhodamine B removal from solution.

2.6. Adsorption studies

Different concentration solutions of metanil yellow and Rhodamine B were respectively contacted with 0.05 g of copper and 0.05 g of Cu–Ni nanoparticles. The working solutions were prepared from the selected dyes stock solutions having 0.0001 M concentration each. The solution pH were adjusted using 0.1 M HCl solution or a dilute (0.1 M) solution of sodium hydroxide as required (pH 5 and 8 were optimum pH respectively for the selected dyes). After shaking for a specific interval of time the adsorbents were removed by filtration and the remaining concentration in solutions were determined using UV-Vis spectrophotometer (437 nm = Rhodamine B and 556 nm = metanil yellow).

2.7. Kinetic adsorption process

In a number of reagent bottles, a fixed concentration solution of metanil and rhodamine dyes were respectively contacted with 0.05 g of mono and bimetallic particles. These bottles were then subjected to shaking for different time intervals (10, 20, 30, 40, 50, and 60 min) at 3 different temperatures of 293, 313, and 333 K. The remaining dyes concentrations were determined.

2.8. Effects of temperature

The effect of temperature on Rhodamine B and metanil yellow was elucidated by contacting fixed concentration solutions of these dyes respectively with mono and bimetallic fabricated particles at different temperature in the range 293 to 333 K. The subsequent experimental detail was same as described.

2.9. pH effect

The way electric charges are distributed on the surface of both the adsorbent and the substance being adsorbed can be affected significantly by acidic or basic environment. The effect of pH was investigated in range from 2 to 12, whereas the other conditions mentioned before were left unchanged.

2.10. Regeneration of adsorbent

The used adsorbents up to 5 cycles were regenerated with acetone and then treating them with NaOH to test how effectively they could be regenerated for in future uses.

3. Results and discussion

3.1. Characterization

3.1.1. Scanning electron microscopy and FTIR spectra of adsorbents

The shape of particles and external appearance of both Cu along with Cu–Ni nanoparticles (NPs) were investigated using the technique of scanning electron microscopy (SEM). Fig. 3a is representing it for Cu NPs whereas Fig. 3b for Cu–Ni NPs. Both adsorbents exhibited rough surfaces with many pores and dispersed particles which are mandatory for adsorption process. The uneven distribution of adsorption sites is a morphological characteristic that could be advantageous for a number of uses, including the adsorption of dyes [10].

The Fourier-transform infrared spectroscopy is a useful tool for characterizing the chemical functional groups found on the surfaces of adsorbents. Fig. 3c and d represent the FTIR spectrum of Cu and Cu–Ni NPs. Though there are peaks around 3,800 and 3,500 cm^{-1} in both the spectrum but may be originated from organic solvent used as medium in hydride solution. These graphs revealed some unique signals. For Cu nanoparticles, there's a distinct signal around 600 cm^{-1}. For Cu–Ni nanoparticles, there are two peaks, one at around 605 cm^{-1} and another at 425 cm^{-1}. These signals confirm the presence of CuO and NiO on the surfaces of the nanoparticles [11].

3.1.2. Energy-dispersive X-ray (EDX)

The energy-dispersive X-ray (EDX) spectra of copper and copper–nickel nanoparticles are respectively shown in Fig. 4a and b. The Cu NPs have 11.64% oxygen indicates that the copper on surface has oxidized. The Cu–Ni NPs also showed 22.81% oxygen, which suggests a similar oxidation mechanism. In the bimetallic NPs nickel constitutes 51.80% and copper accounts for 25.39%.

3.1.3. X-ray diffraction (XRD) pattern

The X-ray diffraction images of copper (Cu) and copper–nickel (Cu–Ni) are shown in Fig. 5a and b, respectively.

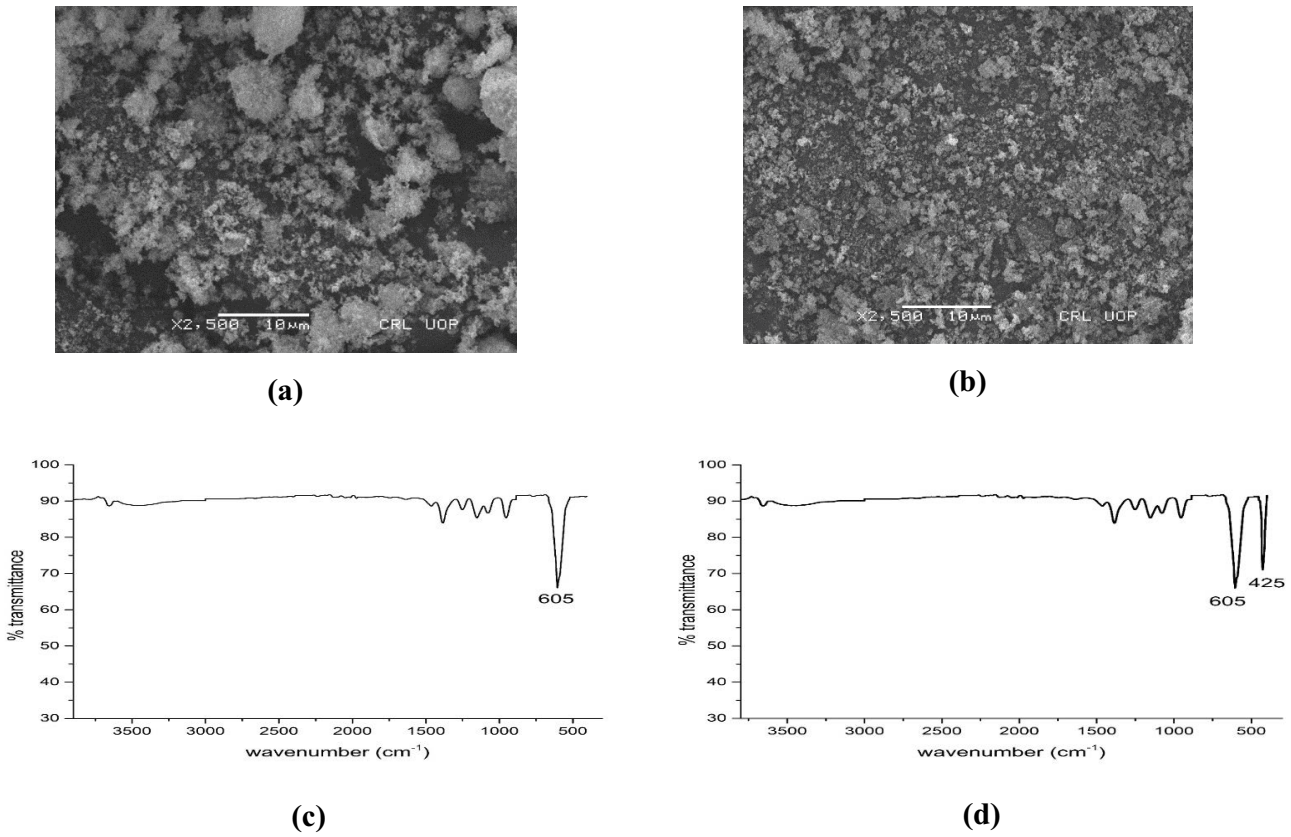

Fig. 3. SEM images (a) and (b) of monometallic and bimetallic nanoparticles. FTIR spectra (c) and (d).

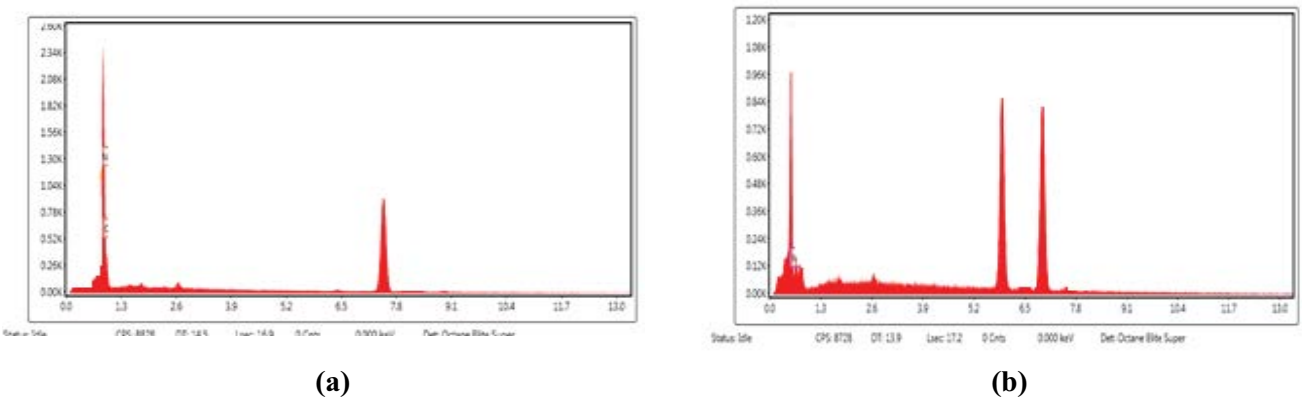

Fig. 4. EDX spectra of monometallic (a) and bimetallic (b) nanoparticles.

The Scherer formula was used to calculate the crystallite's sizes, which showed that it was 6 nm for Cu and 2 nm with Cu–Ni NPs. In addition, it was noted that 83% of the total crystals in Cu–Ni showed crystallinity, compared to 75% in Cu NPs that were crystalline. Crystallinity is correlated with the magnitude of diffraction peaks because the size of crystallites, and diffraction patterns provide an understanding of the arrangement of atoms within the crystal lattice. Understanding the properties and behavior of Cu and Cu–Ni in diverse applications requires knowledge of the structure of the crystal and size, which was provided by the XRD study. The existence of Cu–Ni in bimetallic NPS was confirmed by the diffraction peaks at 2θ values of 39°, 42°, and 73°, which coincide with previously reported literature [11–13].

3.2. Adsorption kinetics

Adsorption kinetics involves the investigation of how quickly adsorption occurs and the factors influencing this process. It encompasses the study of the time-dependent behavior of adsorption, specifically the rate at which an

adsorbate attaches to the surface of adsorbent. A comprehensive understanding of adsorption mechanisms requires a thorough examination of adsorption kinetics. Scientists may learn a lot about the underlying mechanisms regulating adsorption, such as mass transportation, diffusion, the interface reactions, by studying kinetics [14]. Fig. 6a shows the effect of contact time on adsorption of metanil by copper mono NPS whereas Fig. 6b shows it for Rhodamine B on bimetallic NPs. The equilibrium time estimated was 30 min for metanil on Cu NPs whereas 12 min for Rhodamine B on Cu–Ni NPs.

3.2.1. Pseudo-first-order equation

The pseudo-first-order kinetic equation is expressed in its linear form as:

$$\log\left(q_e - q_t\right) = \log q_e - \frac{k_1}{2.303} \tag{1}$$

where k_1 (min^{-1}) represents the equilibrium rate constant of the pseudo-first-order equation. q_e and q_t are the quantity of respective dyes adsorbed at equilibrium and time t. The slope and intercept of the graph $\log(q_e–q_t)$ vs. t is required to determine the variables k_1 and q_e [15]. Fig. 7a and b were used to estimate kinetic constant k_1 values of Rhodamine B on Cu–Ni and metanil yellow on Cu nanoparticles, respectively. The R^2 value was used to decide which model best fit the experimental data. When the R^2 score is very less than 1, it means that the simulation does not completely account for the data's variances and suggests that the model used might not be appropriate for correctly predicting or explaining the sorption processes taking place.

3.2.2. Pseudo-second-order equation

For a process in equilibrium, the pseudo-second-order kinetics equation can be written as:

$$\frac{t}{q_t} = \frac{1}{k_2 q_e^2} + \frac{t}{q_e} \tag{2}$$

where k_2 represents the pseudo-second-order rate constant. The values of q_e (mg/g) and k_2 can be determined from a plot given in Fig. 8 between t/q_t vs. t (the slopes and intercepts) [16]. This model indicated a close match between the predicted and observed equilibrium adsorption capacities (q_e) at all temperatures for both adsorption processes. Additionally, it implies that chemisorption; a process in which the adsorbent and adsorbate form a chemical bond, is occuring at the adsorbent surface. The R^2 values clearly suggest that a pseudo-second-order model more accurate to accomodate the kinetics data.

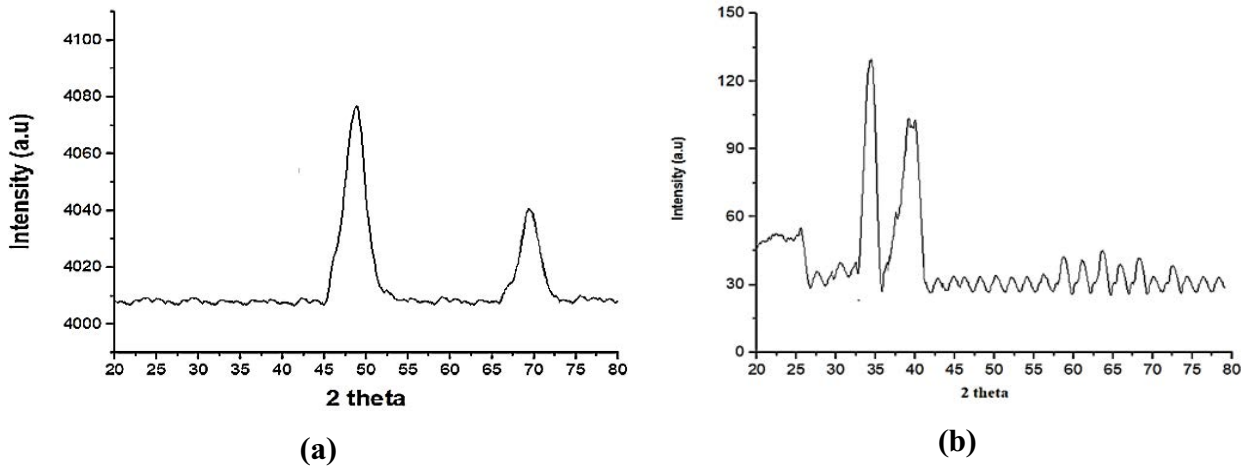

Fig. 5. XRD patterns of monometallic (a) and bimetallic (b) nanoparticles.

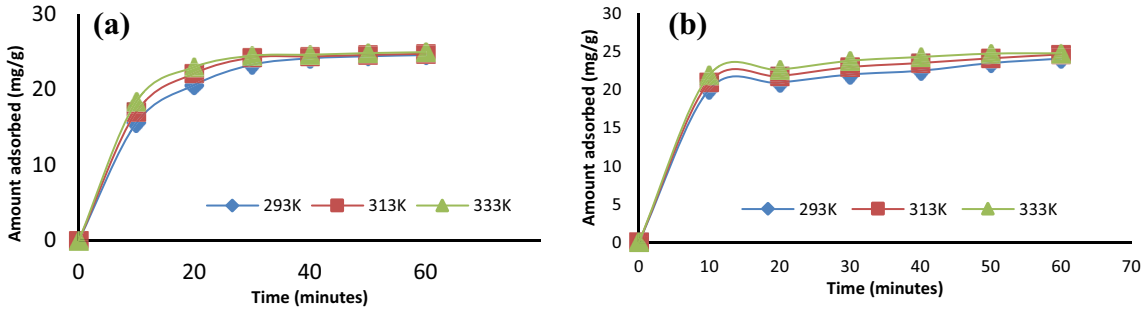

Fig. 6. Effect of time on adsorption of metanil yellow on Cu monometallic (a) and Rhodamine B on Cu–Ni bimetallic (b) nanoparticles.

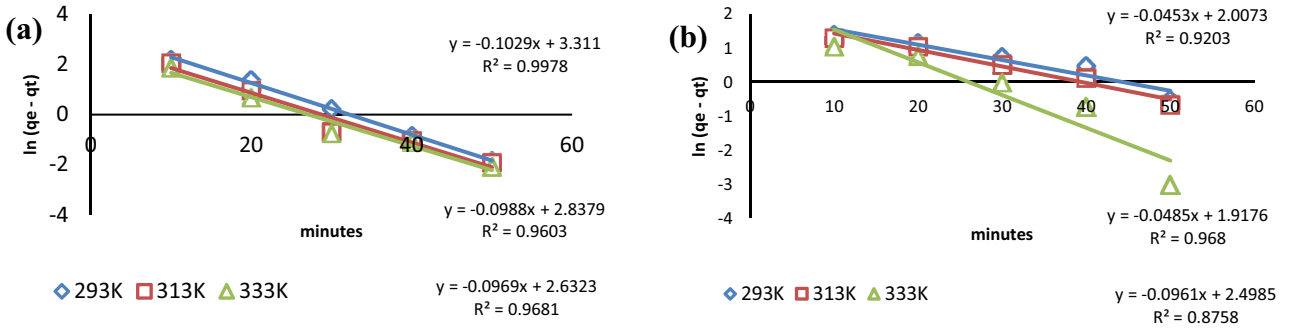

Fig. 7. Pseudo-first-order kinetics for adsorption of metanil yellow on Cu monometallic (a) and Rhodamine B on Cu–Ni bimetallic (b) NPs.

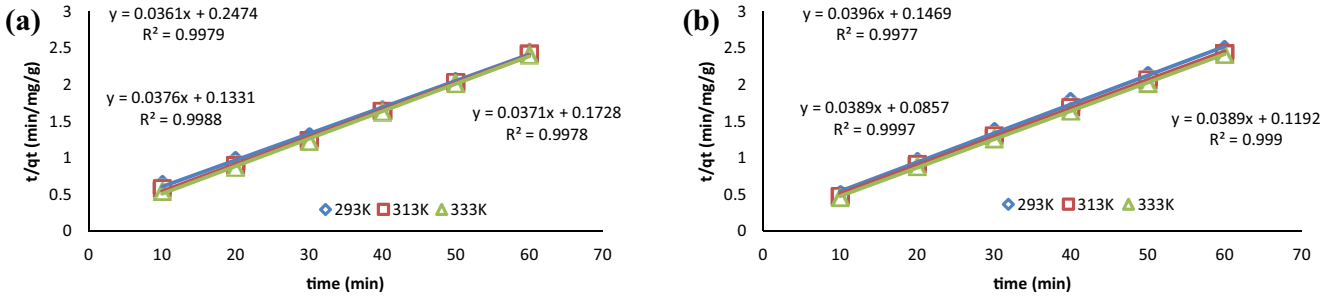

Fig. 8. Linear pseudo-second-order kinetics for adsorption of metanil yellow on Cu monometallic (a) and Rhodamine B on Cu–Ni bimetallic (b) nanoparticles.

3.3. Isotherm studies

To investigate the relationships between adsorbent and adsorbates, Langmuir, the Temkin, and the Freundlich isotherm models are often used. These models provide useful information on the surface characteristics and are helpful in enumerating adsorption capacities. These models are applied to explain the monolayer and multilayer adsorptions occurring of different surfaces [17].

3.3.1. Langmuir isotherm model

Adsorption takes place on a homogenous surface with a limited number of identical sites, as pointed out by this model. It emphasises on the formation of one layer of adsorbate while adsorbing onto a given solid surface. It provides some useful information about the surface energetics, equilibrium constant, and adsorption capacity. The model developed by Langmuir can be expressed mathematically as follows [18]:

$$\frac{C_e}{q_e} = \frac{C_e}{Q_m} + \frac{1}{K_L Q_m} \tag{3}$$

where C_e represents the equilibrium concentration, q_e is the amount adsorbed at equilibrium, K_L is the Langmuir constant, and Q_m is the maximum adsorption capacity. To determine the values of Q_m and K_L, a plot of C_e/q_e vs. C_e was constructed (Fig. 9a–c) for metanil yellow adsorption on Cu NPs and Fig. 9d–f for Rhodamine B on Cu–Ni NPs). The maximum adsorption capacities (Q_m) for metanil yellow on Cu NPs were determined to be 182, 200, and 200 mg/g at temperatures of 293, 313, and 333 K, respectively. Similarly, for Rhodamine B on Cu–Ni NPs, the Q_m values were found to be 357, 370, and 416 mg/g at the respective temperatures. The high R^2 values for this model was very close to one, indicating the appropriateness of this model to accurately describes the adsorption processes.

3.3.2. Freundlich isotherm model

According to the Freundlich isotherm model, different adsorption sites on an uneven surface will experience varied degrees of adsorption. It suggests that when the solute concentration in a solution grows, the adsorption capacity does not remain constant but rather increases. Along with Langmiur model, this is also equally employed to analyse experimental data and describe the adsorption characteristics of various material used as adsorbent. It is crucial to keep in mind that this approach has limits and might not adequately explain adsorption processes in some situations, such as high concentrations of solute or surface saturation. This model can be given as follows:

$$\ln q_e = \ln K_f + \frac{1}{n} \ln C_e \tag{4}$$

where C_e stands for the equilibrium concentration, q_e for the adsorption at a state of equilibrium, K_f for the Freundlich constant, and $1/n$ for the adsorption intensity. The isotherm is regarded as irreversible when $1/n = 0$, favourable when $1/n = 1$, and unfavourable when $1/n > 1$ [19].

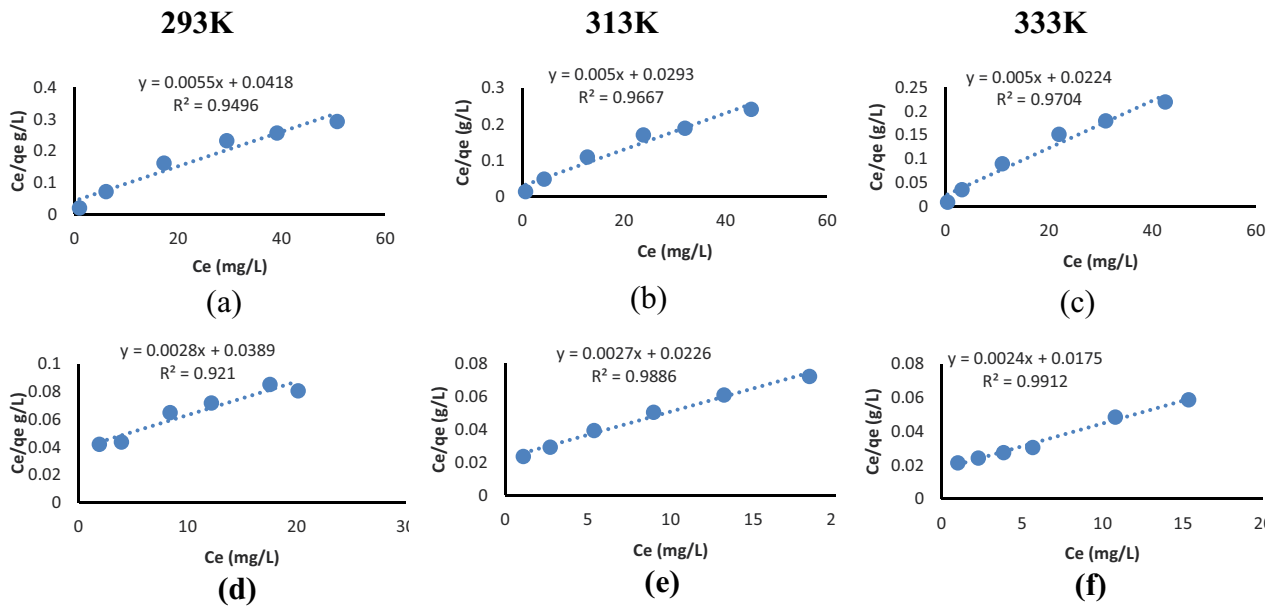

Fig. 9. Langmuir isotherm model for the adsorption of metanil yellow on Cu monometallic (a–c) and Rhodamine B on Cu–Ni bimetallic (d–f) NPs.

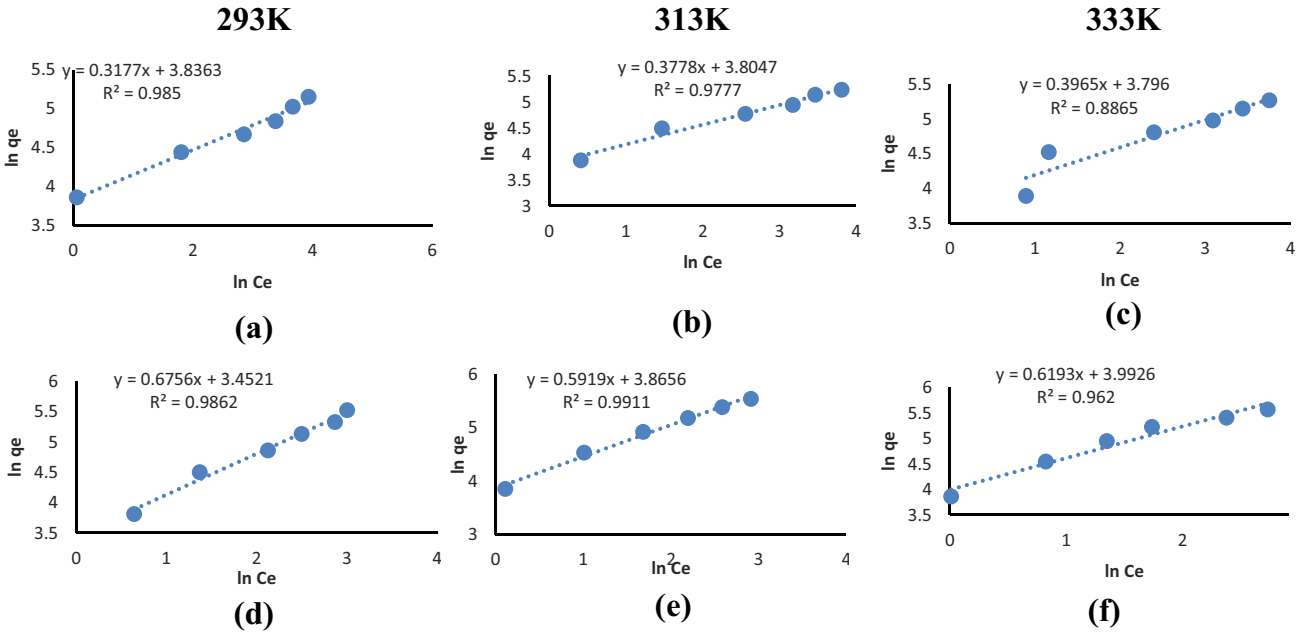

Fig. 10. Freundlich isotherm model for adsorption of metanil yellow on Cu monometallic (a–c) and Rhodamine B on Cu–Ni bimetallic (d–f) NPs.

Plotting ln(q_e) vs. ln(C_e) the obtained graphs in helpful in determining the values of the mentioned parameters from the intercept and slope (Fig. 10a–c) for metanil yellow adsorption on Cu NPs and Fig. 10d–f for Rhodamine B adsorption on Cu–Ni NPs). At temperature of 293, 313, and 333 K, respectively, the 1/*n* coefficients for the adsorption of metanil yellow on Cu were: 0.3177, 0.3778, and 0.3965, whereas of Rhodamine B on Cu–Ni NPs were; 0.6756, 0.5919, and 0.6193.

3.3.3. Temkin isotherm model

According to the Temkin equilibrium model, there are only slight interactions between the molecules of the adsorbate and the solid surface throughout the adsorption process. Further, the adsorbate–adsorbate interactions can cause a drop in capacity for a given adsorbate adsorption as surface coverage rises. It is common practise to analyse experimental data and establish adsorption parameters

using the Temkin isotherm model. Though it offers a good fit for some adsorption systems, it might not be appropriate in all circumstances, particularly where significant adsorbate–adsorbent interactions are prevalent. This model can be expressed mathematically as:

$$q_e = \beta \ln K_T + \beta \ln C_e \quad (5)$$

where β is is the heat of adsorption, and K_T is the equilibrium binding constant, where T is the absolute temperature [20]. Plotting q_e against ln(C_e) these constants were estimated as shown in Fig. 11a–c for the adsorption of metanil yellow on Cu NPs and Fig. 11d–f for the adsorption of Rhodamine B on Cu–Ni NPs.

The R^2 value and its variation in contrast to error analysis were used to evaluate each model's adequacy for describing experimental data. However, the R^2 values for the Langmuir model were closer to 1 inferring that the model to be suitable for explaining isotherm data.

3.4. Effect of pH on % removal

Fig. 12a and b tell us that when the pH of the solution is between 2 and 5, it works best the rate of adsorption was maximum. At this pH range, the surface of the adsorbent becomes positively charged as there were lots of H^+ ions in medium. This positive charge helps in attracting and removing the negatively charged dye molecules. There is a gradual decline in percent removal with increase in pH however, working with acidic pH rather difficult than neutral pH therefore, in this study we have used pH 6 as optimum.

3.5. Thermodynamic study

The following were the thermodynamic equations used to calculate the adsorption parameters:

$$\ln\left(K_c\right) = \frac{\Delta S^\circ}{R} - \frac{\Delta H^\circ}{RT} \quad (6)$$

$$\Delta G^\circ = \Delta H^\circ - T\Delta S^\circ \quad (7)$$

The symbol ΔG° is for the Gibbs free energy, ΔH° is the enthalpy change, ΔS° is entropy change, K_c is the equilibrium constant of adsorption and T is temperature. The intercept and slope values obtained from ln(K_c) vs. 1/T graph can be used to determine the values of ΔH°, ΔG° and ΔS° (Fig. 13).

The spontaneity of the adsorption process was decided from the decrease of Gibbs free energy (ΔG°) at given temperatures, that is, 2.356, 2.117 and 1.878 J/mol for metanil yellow on Cu monometallic nanoparticles and –6.087,

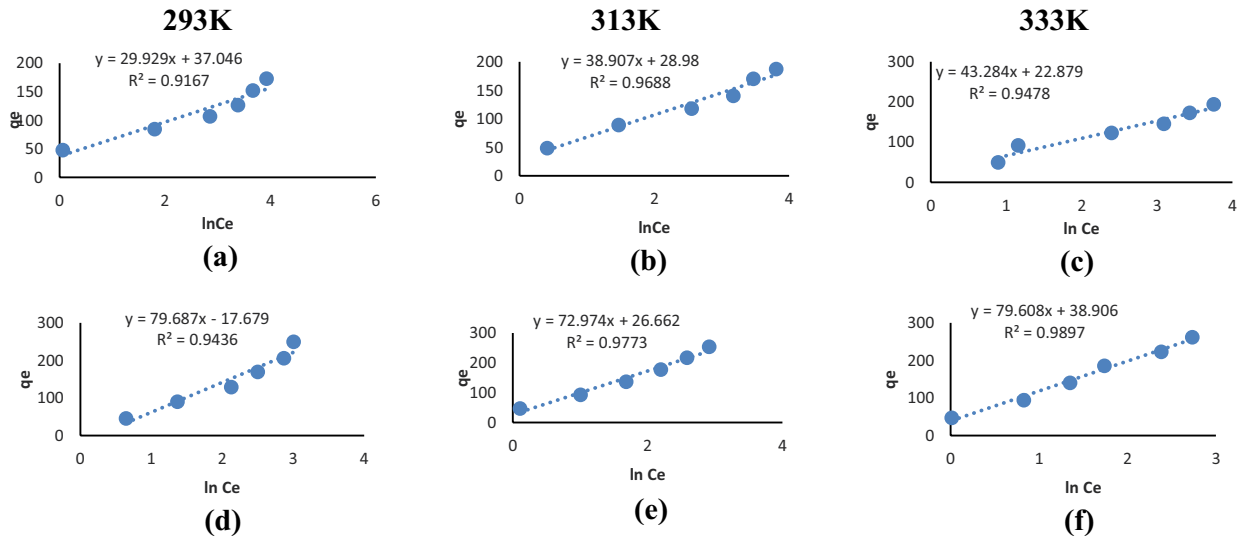

Fig. 11. Temkin isotherms model for adsorption of metanil yellow on Cu monometallic (a) and Rhodamine B on Cu–Ni bimetallic (b) NPs.

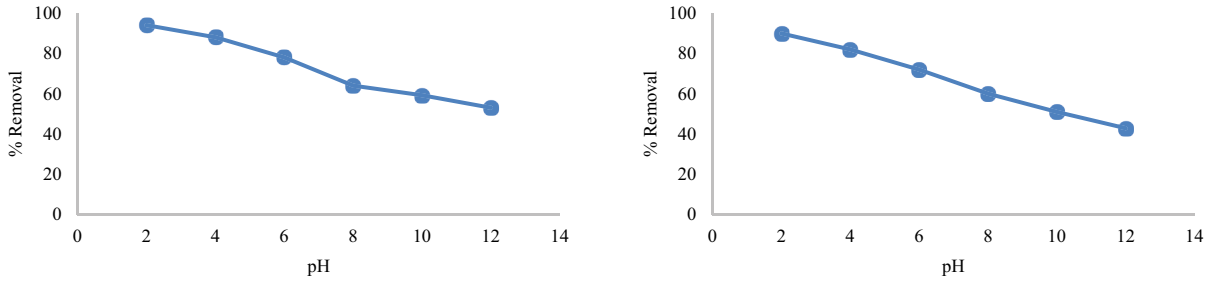

Fig. 12. Effect of pH on % removal of metanil yellow on Cu mono-metallic (a) and Rhodamine B on Cu–Ni bimetallic (b) nanoparticles.

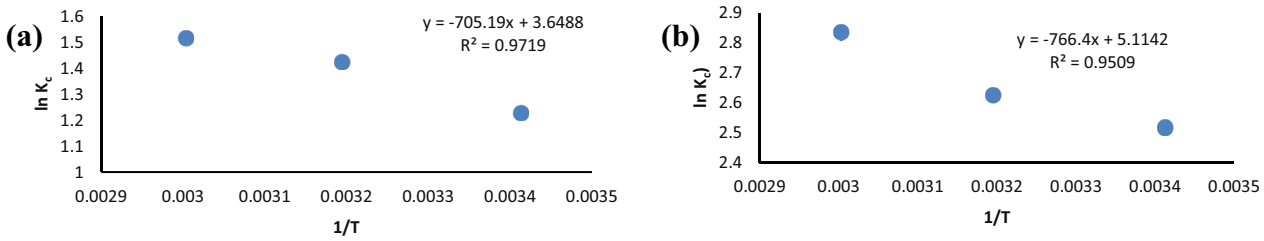

Fig. 13. 1/*T* vs. lnK_c plot for adsorption of metanil yellow on Cu NPs (a) and Rhodamine B on Cu–Ni (b) NPs.

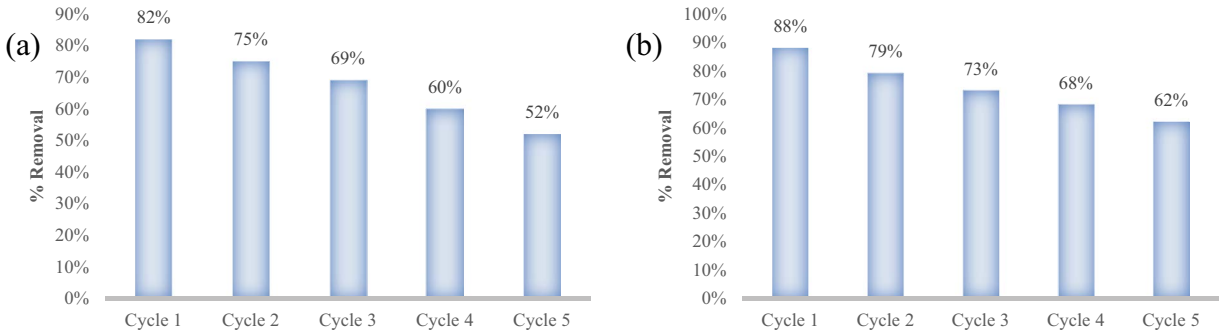

Fig. 14. Cu mono-metallic (a) and Cu–Ni bimetallic nanoparticles reusability and regeneration.

–6.937 and –7.787 J/mol for Rhodamine B on Cu–Ni bimetallic nanoparticles [21] as observed. The positive enthalpy value ($\Delta H°$), that is, 5.861 kJ/mol for metanil yellow on Cu monometallic particles and 6.371 kJ/mol for Rhodamine B on Cu–Ni bimetallic NPs indicates the endothermic nature of the process.

The system gets more stable as adsorption progresses as is clear from positive entropy ($\Delta S°$) 11.96 and 42.519 J/K·mol values respectively for metanil yellow and Rhodamine B on mono and bimetallic particles, that is, there is a rise in disordered at the solid-solution interface [22].

3.6. Regeneration and reusability

The prepared mono and bimetallic particles were subjected to reusability study after contacting with their respective dyes for 5 cycles. Each time regenerated with suitable solvents and reused. Up to 5 cycles the activity still retained was 52% for monometallic NPs and 62% for bimetallic NPs as shown in Fig. 14a and b.

4. Conclusions

From metal salts precursors, monometallic Cu and bimetallic Cu–Ni were prepared and characterized by SEM, EDX, FTIR and XRD. The equilibrium was reached within 30 min for metanil yellow on Cu NPs whereas in the case of Rhodamine B it was established within 12 min. The chemisorption nature both processes was decided from the best fit of kinetics data obtained with pseudo-second-order kinetics model. The adsorption in monolayer was confirmed from best fit obtained with Langmuir isotherm model for the collected isotherm data. The maximum adsorption capacity calculated was 200 mg/g for metanil yellow over Cu NPs and 416 mg/g for Rhodamine B on Cu–Ni NPs. The metanil yellow adsorption onto Cu was found to be endothermic with an enthalpy value of 5.861 kJ/mol whereas it was 6.371 kJ/mol for Rhodamine B adsorption. The Gibs free energy values calculated were; 2.356, 2.117, and 1.878 kJ/mol at 293, 313, and 333 K, respectively and –6.087, –6.937, and –7.787 kJ/mol for Rhodamine B correspondingly. The randomness across the interface between the solid and the solution during the process of adsorption calculated were, 11.96 and 42.519 J/mol·K for metanil yellow and Rhodamine B adsorption on Cu and Cu–Ni NPs, respectively. Both these adsorbents could be used as alternative of activated carbon however, in this regard further studies are required on other pollutant to fully evaluate them for future uses.

Acknowledgment

The authors extend their appreciation to the researchers supporting Project number (RSP2023R110) King Saud University, Riyadh, Saudi Arabia, for financial support.

References

[1] A.U. Khan, M. Zahoor, M.U. Rehman, M. Ikram, D. Zhu, M.N. Umar, R. Ullah, E.A. Ali, Bioremediation of azo dye brown 703 by *Pseudomonas aeruginosa*: an effective treatment technique for dye-polluted wastewater, Microbiol. Res., 14 (2023) 1049–1066.
[2] A. Patel, S. Soni, J. Mittal, A. Mittal, C. Arora, Sequestration of crystal violet from aqueous solution using ash of black turmeric rhizome, Desal. Water Treat., 220 (2021) 342–352.
[3] J. Mittal, permissible synthetic food dyes in India resonance, J. Sci. Educ., 24 (2020) 567–577.
[4] U.K. Sharma, R. Kumar, A. Gupta, R. Ganguly, A.K. Singh, A.K, Ojha, A.K. Pandey, Ameliorating efficacy of eugenol against metanil yellow induced toxicity in albino Wistar rats, Food Chem. Toxicol., 126 (2019) 34–40.
[5] V. Masindi, K.L. Muedi, Environmental contamination by heavy metals, Heavy Metals, 10 (2018) 115–132.

[6] H. Daraei, A. Mittal, Investigation of adsorption performance of activated carbon prepared from waste tire for the removal of methylene blue dye from wastewater, Desal. Water Treat., 90 (2017) 294–298.
[7] M. Sadia, I. Ahmad, Z.U. Saleheen, M. Zubair, M. Zahoor, R. Ullah, A. Bari, I. Zekker, Synthesis and characterization of MIPs for selective removal of textile dye Acid Black-234 from wastewater sample, Molecules, 28 (2023) 1555, doi: 10.3390/molecules28041555.
[8] Q. Khan, M. Zahoor, S.M. Salman, M. Wahab, M. Talha, A.W. Kamran, Y. Khan, R. Ullah, E.A. Ali, A.B. Shah, The chemically modified leaves of *Pteris vittata* as efficient adsorbent for zinc(II) removal from aqueous solution, Water, 14 (2022) 4039, doi: 10.3390/w14244039.
[9] M. Ikram, M. Naeem, M. Zahoor, A. Rahim, M.M. Hanafiah, H.M. Oyekanmi, A.B. Shah, M.H. Mahnashi, A.A. Ali, N.A. Jalal, F. Banthun, A. Sadiq, Biodegradation of azo dye methyl red by *Pseudomonas aeruginosa*: optimization of process conditions, Int. J. Environ. Res. Public Health, 19 (2022) 9962, doi: 10.3390/ijerph19169962.
[10] K.B. Tan, M. Vakili, B.A. Horri, P.E. Poh, A.Z. Abdullah, B. Salamatinia, Adsorption of dyes by nanomaterials: recent developments and adsorption mechanisms, Sep. Purif. Technol., 150 (2015) 229–242.
[11] Q. Li, Y. Wang, C. Chang, Study of Cu, Co, Mn and La doped NiZn ferrite nanorods synthesized by the coprecipitation method, J. Alloys Compd., 505 (2010) 523–526.
[12] S. Sun, H. Zeng, D.B. Robinson, S. Raoux, P.M. Rice, S.X. Wang, G. Li. Monodisperse MFe_2O_4 (M = Fe, Co, Mn) nanoparticles, J. Am. Chem. Soc., 126 (2004) 273–279.
[13] A. da Silva, N. Bion, F. Epron, S. Baraka, F. Fonseca, R. Rabelo-Neto, L. Mattos, F. Noronha, Effect of the type of ceria dopant on the performance of Ni/CeO_2 SOFC anode for ethanol internal reforming, Appl. Catal., B, 206 (2017) 626–641.
[14] M. Ghaedi, A. Ansari, M. Habibi, A. Asghari, Removal of malachite green from aqueous solution by zinc oxide nanoparticle loaded on activated carbon: kinetics and isotherm study, J. Ind. Eng. Chem., 20 (2014) 17–28.
[15] H.N. Tran, S.J. You, A. Hosseini-Bandegharaei, H.P. Chao, Mistakes and inconsistencies regarding adsorption of contaminants from aqueous solutions: a critical review, Water Res., 120 (2017) 88–116.
[16] M. Ghaedi, A. Ansari, R. Sahraei, ZnS:Cu nanoparticles loaded on activated carbon as novel adsorbent for kinetic, thermodynamic and isotherm studies of Reactive Orange 12 and Direct yellow 12 adsorption, Acta A Mol. Biomol., 114 (2013) 687–694.
[17] M. Saxena, N. Sharma, R. Saxena, Highly efficient and rapid removal of a toxic dye: adsorption kinetics, isotherm, and mechanism studies on functionalized multiwalled carbon nanotubes, Surf. Interfaces, 21 (2020) 100639, doi: 10.1016/j.surfin.2020.100639.
[18] I. Langmuir, The adsorption of gases on plane surfaces of glass, mica and platinum, J. Am. Chem. Soc., 40 (1918) 1361–1403.
[19] H. Freundlich, Over the adsorption in solution, J. Phys. Chem., 57 (1906) 1100–1107.
[20] V.S. Munagapati, D.S. Kim, Equilibrium isotherms, kinetics, and thermodynamics studies for Congo red adsorption using calcium alginate beads impregnated with nano-goethite, Ecotoxicol. Environ. Saf., 141 (2017) 226–234.
[21] C. Namasivayam, S. Senthilkumar, Recycling of industrial solid waste for the removal of mercury(II) by adsorption process, Chemosphere, 34 (1997) 357–375.
[22] E.C. Lima, A.A. Gomes, H.N. Tran, Comparison of the nonlinear and linear forms of the van't Hoff equation for calculation of adsorption thermodynamic parameters ($\Delta S°$ and $\Delta H°$), J. Mol. Liq., 311 (2020) 113315, doi: 10.1016/j.molliq.2020.113315.